

## Thiopental-Inspired alkylpyrimidines as dual-target antimicrobial agents: Synthesis, biological activity, and molecular docking validation

Mahmoud M. Hamed<sup>a</sup>, Mostafa Ahmed<sup>a</sup>, Adel M. Kamal El-Dean<sup>b</sup>, M. Yasser Alsedfy<sup>c,d</sup> and Mahmoud S. Tolba<sup>a\*</sup>

<sup>a</sup>Chemistry Department, Faculty of Science, New Valley University, El-Kharja 72511, Egypt

<sup>b</sup>Chemistry Department, Faculty of Science, Assiut University, Assiut 71516, Egypt

<sup>c</sup>Department of Radiology, Faculty of Applied Health Sciences, Sphinx University, New Assiut, Egypt

<sup>d</sup>Egyptian Cancer Research Network, Academy of Scientific Research and Technology, Cairo, Egypt

### CHRONICLE

#### Article history:

Received March 12, 2025

Received in revised form

June 5, 2025

Accepted August 5, 2025

Available online

August 5, 2025

#### Keywords:

Thiopental derivatives

Antimicrobial agents

Pyrimidine hybrids

Molecular docking

Structure-activity

relationships (SARs)

CYP51 inhibition

### ABSTRACT

Alkylpyrimidine derivatives, particularly thiopental-based analogs, have emerged as promising scaffolds for antimicrobial drug development. In this study, we designed and synthesized a series of novel thiopental-pyrimidine hybrids (**3a–c**, **4**) through efficient condensation reactions, and characterized these compounds by using NMR, IR, and mass spectrometry. Antimicrobial screening revealed significant activity against clinically relevant strains: derivative **3a** exhibited selective inhibition of *Bacillus subtilis* (MIC: 10.5±0.4 mg/mL) and *Escherichia coli* (MIC: 22.1±0.3 mg/mL), while **3c** showed potent antifungal effects against *Candida albicans* (MIC: 11.6±0.4 mg/mL). Molecular docking studies elucidated the mechanistic basis of this activity, with **3a** binding to penicillin-binding protein (PBP; −6.4 kcal/mol) via hydrogen bonds (SER392) and hydrophobic interactions (TYR430, PRO660), and **3c** coordinating with the heme iron of CYP51 (−7.8 kcal/mol) akin to fluconazole. Notably, **3c** thioether linkage facilitated  $\pi$ -cation/anion interactions with PHE463, rationalizing its antifungal specificity. Structure-activity relationships (SAR) underscored the critical roles of electron-deficient pyrimidine cores for antibacterial activity and sulfur moieties for antifungal action. These findings position thiopental-pyrimidine hybrids as versatile leads for combating microbial resistance, with **3c** representing a particularly promising antifungal candidate. Our integrated synthetic, biological, and computational approach provides a blueprint for optimizing these scaffolds for clinical translation.

© 2025 by the authors; licensee Growing Science, Canada.

## 1. Introduction

Organic compounds are fundamental to life and underpin a vast array of industrial and technological advancements.<sup>1–11</sup> Their structural diversity allows for an astonishing range of chemical properties and functions, making them indispensable in different fields such as medicine, agriculture and other fields.<sup>12–22</sup> Within this expansive domain, heterocyclic compounds – organic molecules containing at least one non-carbon atom within their ring structure – represent a vital subclass due to the unique reactivity and biological activity.<sup>23–34</sup> Among these, pyrimidine-based compounds are of immense significance, featuring a six-membered aromatic ring with two nitrogen atoms. Specifically, alkyl pyrimidines, where hydrocarbon chains are attached to the pyrimidine core and often improved interactions with biological targets.<sup>35–37</sup> Alkyl pyrimidines are a significant class of heterocyclic compounds that have garnered considerable attention in medicinal chemistry, drug discovery, and materials science due to their diverse biological activities and structural versatility.<sup>38–40</sup> The pyrimidine nucleus, serves as a fundamental scaffold in numerous biomolecules, including nucleic acids (uracil, thymine, and cytosine), vitamins (thiamine), and coenzymes (FAD and NADP).<sup>41</sup> The introduction of alkyl substituents onto the pyrimidine ring

\* Corresponding author

E-mail address [mahmoud.tolba@sci.nvu.edu.eg](mailto:mahmoud.tolba@sci.nvu.edu.eg) (M. S. Tolba)

enhances lipophilicity, modulates electronic properties, and improves pharmacokinetic profiles, making alkyl pyrimidines crucial in pharmaceutical applications.<sup>42</sup>

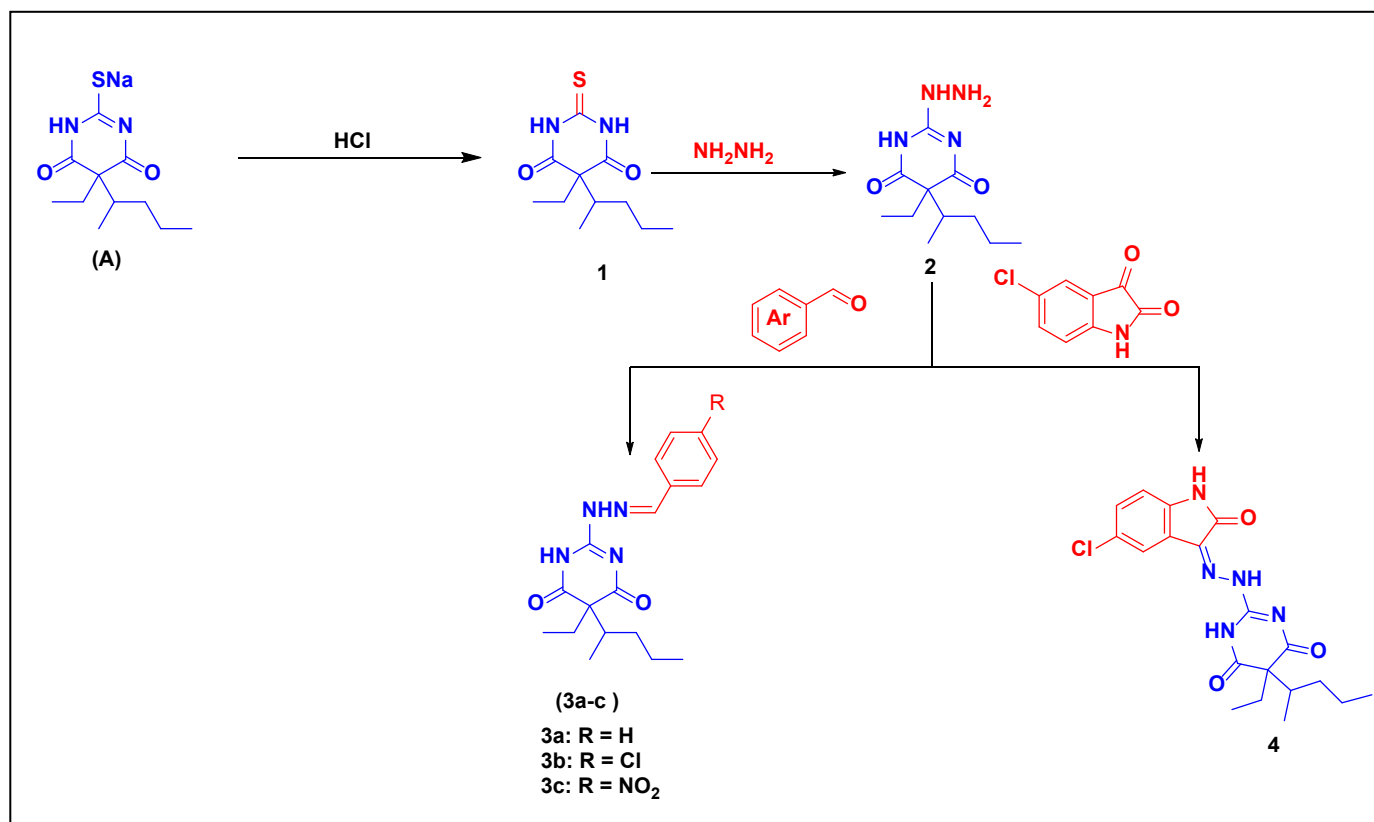
In medicinal chemistry, alkyl pyrimidine derivatives exhibit a broad spectrum of pharmacological activities, including antimicrobial,<sup>43</sup> anticancer,<sup>44,45</sup> antiviral<sup>46</sup> and anti-inflammatory effects<sup>47</sup>. For instance, 5-fluorouracil (5-FU), a fluorinated pyrimidine analog, remains a cornerstone in chemotherapy for treating colorectal and breast cancers.<sup>48</sup> Similarly, trimethoprim, an alkyl diaminopyrimidine, is widely used as an antibacterial agent by inhibiting bacterial dihydrofolate reductase.<sup>42</sup> Recent studies have also highlighted the role of alkyl pyrimidines in kinase inhibition, with compounds such as imatinib (containing a pyrimidine core) being effective against chronic myeloid leukemia.<sup>43</sup> Beyond therapeutics, alkyl pyrimidines find applications in agrochemicals as fungicides and herbicides.<sup>49,50</sup> Their ability to interact with biological targets, such as enzymes and receptors, makes them valuable in crop protection.

Additionally, alkyl pyrimidines are employed in materials science, particularly in the synthesis of organic semiconductors and luminescent materials due to their electron-deficient aromatic system.<sup>51</sup> Thiopental is an Alkyl Pyrimidine Derivative with Anesthetic and anti microbial Applications Among the clinically significant alkyl pyrimidines.<sup>52,53</sup> Although thiopental is primarily recognized as an anesthetic, emerging studies suggest its potential as an antimicrobial agent, particularly against drug-resistant pathogens. The thiobarbiturate core of thiopental, structurally derived from pyrimidine, exhibits moderate antibacterial and antifungal activity by interfering with microbial DNA replication and membrane integrity.<sup>54</sup> Research indicates that thiopental and its analogs can inhibit the growth of *Candida albicans* and *Aspergillus fumigatus* by disrupting fungal ergosterol biosynthesis, a mechanism akin to azole antifungals.<sup>55</sup> Additionally, thiopental derivatives have demonstrated bacteriostatic effects against Gram-positive bacteria, including *Staphylococcus aureus*, possibly through interaction with bacterial topoisomerases.<sup>56</sup> While its clinical use as an antimicrobial remains exploratory, structural modifications of thiopental's pyrimidine-thiobarbiturate scaffold could yield novel broad-spectrum agents, especially in an era of rising antimicrobial resistance.<sup>57</sup> Building upon our ongoing research efforts,<sup>58-60</sup> this manuscript is dedicated to the design and optimization of efficient synthetic strategies for thiopental-based alkylpyrimidine derivatives. Furthermore, we explore their therapeutic potential in medicinal chemistry, with particular emphasis on their promising applications as novel antimicrobial agents.

## 2. Result and Discussion

### 2.1. Chemistry

The modification of the thiopental compound begins with a sodium thiopental derivative that undergoes acidic treatment with HCl, to obtain a thiol group for subsequent reactions. This reaction successfully delivered 5-ethyl-5-(pentan-2-yl)-2-thioxodihydropyrimidine-4,6-(1*H*,5*H*)-dione (**1**).<sup>61</sup> The intermediate **1** reacts with hydrazine hydrate (NH<sub>2</sub>NH<sub>2</sub>.H<sub>2</sub>O) in one step to produce hydrazinyl derivative **2**, likely undergoing hydrazine substitution to form amine derivatives, modifying the electron density around the core. Subsequent the condensation of hydrazinyl compound **2** with aromatic aldehydes or isatin furnished the derivatives **3a-c** and **4**, respectively. The synthetic intermediates and final products are then characterized by standard analytical techniques, such as NMR, mass spectrometry, and IR spectroscopy, to confirm the incorporation of desired functional groups, purity, and molecular structure. The reaction mechanism generally precedes via nucleophilic attack, electrophilic substitution, or condensation, with hydrazine acting as a nucleophile that tailor the compound's pharmacological profile. The IR of compound **1** showed new vibrational bands at 3264, 3154, 1671, and 1735 cm<sup>-1</sup> for two NH groups, and two C=O groups respectively. While the <sup>1</sup>H NMR spectrum exhibited distinctive signals for the aliphatic protons at 0.71, 0.82, 0.91, 1.06, 1.37, 1.89, 2.02 ppm, respectively and 2NH groups at 12.61 ppm, while its <sup>13</sup>C NMR showed signals at δ 0.91, 9.50, 12.49 ppm, respectively for 3CH<sub>3</sub> groups, and at δ 19.89, 27.19, 32.23 ppm, respectively for CH<sub>2</sub> groups, CH appear at δ 41.23 ppm, at δ 58.96 ppm =C= pyrimidine, signal which distinguish for 2C=O groups at δ 169.96, 170.25 ppm, respectively. Presented of distinctive signals for C=S at δ 178.62 ppm. Formation of compound **2** was established by FT-IR, <sup>1</sup>H-NMR and <sup>13</sup>C-NMR spectra. FT-IR spectrum of compound **2** exhibited absorption bands at 3344 cm<sup>-1</sup> for NH<sub>2</sub> group. <sup>1</sup>H NMR spectrum showed the presence of broad signal at δ 7.76 ppm attributed to NH and NH<sub>2</sub> protons. While, its <sup>13</sup>C-NMR spectrum showed the disappearance of the characteristic peak of the thiol group. The structural characterization of compounds **3a-d** was confirmed through comprehensive spectroscopic analysis. Compound **3a** showed an aromatic C-H stretch at 3044 cm<sup>-1</sup> in its FT-IR spectrum, while its <sup>1</sup>H-NMR spectrum displayed characteristic signals including a singlet at δ 8.34 ppm (CH), aromatic multiplets (δ 7.00-8.20 ppm), and NH protons at δ 11.35 ppm. The <sup>13</sup>C NMR spectrum of **3a** revealed key signals at δ 155.57 ppm (CH) and aromatic carbons between δ 127.49-134.20 ppm. Similarly, compound **3b** exhibited analogous <sup>1</sup>H-NMR patterns with NH protons at δ 11.46 ppm and <sup>13</sup>C-NMR signals at δ 155.30 ppm (CH) and δ 128.26-135.57 ppm (aromatic carbons). Compound **3c** demonstrated an aromatic C-H stretch at 3066 cm<sup>-1</sup>, with <sup>1</sup>H-NMR signals at δ 8.47 ppm (CH), δ 8.00-8.40 ppm (aromatic protons), and δ 11.49 ppm (NH), supported by <sup>13</sup>C-NMR signals at δ 152.96 ppm (CH) and δ 123.13-140.53 ppm (aromatic carbons). For compound **4**, the FT-IR spectrum showed three carbonyl stretches (1666, 1691, 1718 cm<sup>-1</sup>), while its <sup>1</sup>H NMR spectrum featured aromatic multiplets (δ 6.50-7.50 ppm) and three NH singlets (δ 8.51, 10.85, 12.37 ppm). The <sup>13</sup>C-NMR spectrum of **4** confirmed the structure through aromatic carbon signals (δ 112.22-142.64 ppm) and distinctive peaks at δ 146.27 ppm (C=N) and δ 172.69 ppm (C=O), collectively verifying the successful synthesis of all target compounds.



**Scheme 1.** Synthesis of the target 5-ethyl-2-hydrazinyl-5-(pentan-2-yl)pyrimidine-4,6(1H,5H)-dione derivatives (2-4).

## 2.2. Biological Activity

### 2.2.1. Anti-microbial Activity

The antimicrobial evaluation and molecular docking studies provide compelling insights into the structure-activity relationships (SAR) of the synthesized alkylpyrimidine derivatives, particularly **3a** and **3c**. The experimental MIC values (**Table 1**) and computational binding analyses (**Figs. 1–4**) collectively reveal how structural features govern biological activity against bacterial and fungal targets. Derivative **3a** exhibited selective activity against *Bacillus subtilis* (MIC: 10.5±0.4 mg/mL) and *Escherichia coli* (MIC: 22.1±0.3 mg/mL), while showing no effect on *Staphylococcus aureus* or *Pseudomonas aeruginosa*. This selectivity aligns with its moderate binding affinity (-6.4 kcal/mol) to PBP (PDB: 3VSL), as revealed by docking studies. The electron-deficient pyrimidine core of **3a** formed key interactions with SER392 (hydrogen bond) and hydrophobic residues (TYR430, PRO660), albeit fewer than cefotaxime (-7.9 kcal/mol), which formed 14 bonds, including salt bridges with GLU623/LYS618. This explains **3a**'s narrower spectrum compared to cefotaxime, which targets multiple PBPs broadly. The inactivity of **3b** and **4** may stem from steric bulk or lack of polar groups, hindering PBP access—a hypothesis supported by their absence of docking interactions.

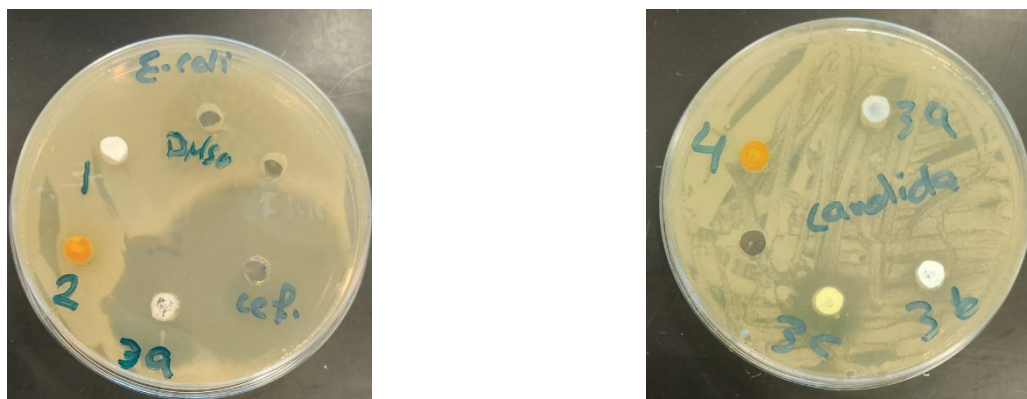
Derivative **3c** demonstrated notable activity against *Candida albicans* (MIC: 11.6±0.4 mg/mL), mirroring its high binding affinity (-7.8 kcal/mol) to CYP51 (PDB: 5V5Z). Critically, **3c**'s thioether-linked pyrimidine coordinated with the heme iron (2.4 Å distance), akin to fluconazole's triazole-iron interaction (2.9 Å). This mimics the mechanism of azole antifungals, where heme coordination disrupts ergosterol biosynthesis. The additional  $\pi$ -cation/ $\pi$ -anion bonds with PHE463 and hydrophobic interactions with CYS470/ALA476 (**Fig. 2**) suggest enhanced stability, justifying its potency. In contrast, derivatives lacking thioether moieties (e.g., **1**, **2**) showed no activity, underscoring the essential role of sulfur in antifungal targeting.

### Structure-activity relationships (SARs) and Design Implications

**Gram-positive vs. Gram-negative activity:** The limited Gram-negative activity of **3a** (only *E. coli*) may reflect efflux pump evasion or partial outer membrane penetration, whereas its Gram-positive activity aligns with PBP accessibility. **Antifungal specificity:** **3c**'s selectivity for *C. albicans* over bacteria highlights the scaffold's adaptability; thioether groups favor CYP51 over bacterial targets.

**Table 1.** The MIC values of the tested derivative against the tested microbial standard strains.

Standard strains	MIC	Gram positive Strains			Gram negative strains		Yeast
		<i>Staphylococcus aureus</i> ATCC 6538	<i>Bacillus subtilis</i> ATCC 6633	<i>Pseudomonas aeruginosa</i> ATCC 9027	<i>Escherichia coli</i> ATCC 25416	<i>Candida albicans</i> ATCC 10231	
Derivatives							
<b>1</b>	10 mg/mL	0	0	0	0	0	
<b>2</b>		09.2±0.3	0	0	0	0	
<b>3a</b>		0	10.5±0.4	0	22.1±0.3	0	
<b>3b</b>		0	0	0	0	0	
<b>3c</b>		0	0	0	0	11.6±0.4	
<b>4</b>		0	0	0	0	0	
<b>Cefotaxime</b>		38.1±0.1	37.3±0.3	27.1±0.4	36.2±0.5	----	
<b>Fluconazole</b>	----	----	----	----	29.2±0.3		
<b>DMSO</b>	0	0	0	0	0		

**Fig. 1.** demonstrates the inhibitory activity of compounds **3a** (vs. *E. coli*) and **3c** (vs. *C. albicans*).

### 2.2.2. Docking studies

Molecular modeling studies are highly valued and recommended to visualize the binding mode and to predict the binding affinity and how the tested compounds could interact with the active site of target proteins,<sup>62</sup> accordingly molecular docking was performed against one bacterial protein and one fungal protein which are already well recognized as crucial targets for antibacterial and antifungal agents. It is highly recommended to validate molecular docking procedure to ensure reliability and credibility of results,<sup>63</sup> so we performed a redocking for cefotaxime and fluconazole to the initial geometric position of each crystal in the X-ray crystallographic protein–crystal complex structure. The validation of molecular docking results obtained by CB-DOCK 2 revealed that the binding modes were almost identical for cefotaxime and fluconazole on the original crystal sites with RMSD 0.62 Å and 0.43 Å respectively, as shown in figures 5. The binding interactions of compound **3a** and cefotaxime as control against bacterial protein penicillin binding protein (PDB 3VSL) are shown in figures 1 and 3. Penicillin-binding proteins (PBPs) are critical enzymes in bacterial cell wall synthesis, specifically responsible for cross-linking peptidoglycan stem peptides during peptidoglycan assembly. These proteins are targeted by  $\beta$ -lactam antibiotics, such as penicillin and cefotaxime which is a third-generation cephalosporin antibiotic that exerts its bactericidal activity by binding to penicillin-binding proteins (PBPs) and inhibiting the transpeptidation step essential for peptidoglycan cross-linking in bacterial cell walls. This inhibition disrupts cell wall synthesis, leading to bacterial cell lysis. Cefotaxime shows high affinity for multiple PBPs, including PBP1b and PBP3, contributing to its broad-spectrum activity against both Gram-positive and Gram-negative bacteria.<sup>64,65</sup> As represented in **Figs. (2), (4)** and **Table 2**, the tested compound has shown a binding affinity of -6.4 kcal/mol while the positive control cefotaxime was -7.9 kcal/mol, The binding affinity values from our docking study indicate that cefotaxime exhibits stronger interaction with the target compared to our tested compound **3a**, because a more negative binding energy typically correlates with higher binding stability, this may explain why cefotaxime is a wide spectrum antibiotic which affected all tested bacteria strains while our compound affected only two strains of the four tested strains despite potency. Focusing on interactions we can see that **3a** made 6 bonds as following, one hydrogen bond with SER 392, three alkyl bonds with TYR 430, PRO 660, one pi-alkyl bond with ILE 522 and one carbon-hydrogen bond with SER 448, while cefotaxime made 14 bonds as following, six hydrogen bonds with SER 448, THR 621, THR 619, GLU 623, GLN 524, three salt bridge bonds with GLU 623, LYS 618 and five carbon-hydrogen bonds with GLU 623, GLY 620, SER 392, THR 621 residues of penicillin binding protein active site, this could explain why cefotaxime got a higher binding affinity than the tested compound **3a**, this came in agreement with recent studies as discussed in details<sup>66</sup>. Cytochrome P450 (CYP) enzymes are pivotal targets for antifungal therapies due to their essential roles in fungal survival and pathogenicity. The most well-characterized target is CYP51 (lanosterol 14 $\alpha$ -demethylase), which catalyzes a critical step in ergosterol biosynthesis – a key component of fungal cell membranes. Azole antifungals (e.g., fluconazole, voriconazole) inhibit CYP51 by binding to its heme cofactor, disrupting membrane

integrity and leading to cell death.<sup>67,68</sup> Our tested compound **3c** shown a high affinity of binding (-7.8 kcal/mol) toward the active site of fungal protein P450, while fluconazole got a binding score of -8.9 kcal/mol, by further analysis of binding mode and interactions as represented in **Figs. (3), (5)** and **Table (2)**, we can find that compound **3c** made ten bonds with the active site of P450 which contains heme, 1 pi anion bond with PHE 463, one pi cation bond with PHE 463, 2 pi alkyl bonds with CYS 470, ALA 476, 4 alkyl bonds with LYS 143, ILE 471, ILE 131, 1 carbon hydrogen bond with PRO 375 and finally 1 pi donor hydrogen bond with CYS 470. Coming to fluconazole it bounded to P450 active site containing heme through seven bonds as following, one halogen bond between fluorine and GLY 303, 4 pi-alkyl bonds with LEU 121, MET 508, LEU 376, ILE 131, 1 pi-sigma bond with THR 311, 1 bond of pi-pi T shaped TYR 118, 1 carbon-hydrogen bond with GLY 307 residue, many previous studies reported that azole interacts via hydrophobic contacts with residues near the heme pocket (including methionine, leucine, and glycine residues) that stabilize binding<sup>69</sup>. The most important interaction which is considered the key player in all azole compounds including Fluconazole that it inhibits fungal growth by targeting cytochrome P450 enzyme CYP51 (lanosterol 14 $\alpha$ -demethylase), which is essential for ergosterol biosynthesis. Its triazole ring coordinates with the heme iron in CYP51's active site, blocking the conversion of lanosterol to ergosterol. This disruption leads to toxic methylated sterol accumulation and impaired cell membrane integrity, ultimately causing fungal cell death,<sup>70</sup> interestingly our docking results of the compound **3c** and fluconazole came in agreements with previous reports<sup>71</sup>, as shown in **Fig. (3)**, the nitrogen atom in position 3 of pyrimidine ring coordinated with iron atom in heme with distance of 2.4 Å, while nitrogen atom of triazole ring in fluconazole coordinated perpendicularly with iron atom in heme with distance of 2.9 Å as shown in **Fig. (5)**, these results strongly support our in vitro results in the context of **3c** antifungal effect.

In summary, the in silico molecular docking studies presented herein provide robust mechanistic insights into the binding interactions and affinities of our synthesized compounds **3a** and **3c** against clinically relevant bacterial and fungal protein targets. By employing validated docking protocols and benchmarking against established drugs (cefotaxime and fluconazole), we ensured the reliability and relevance of our computational results. The detailed analysis of binding modes and key molecular interactions not only corroborates the observed in vitro activities but also highlights the potential of compound **3c** as a promising antifungal agent, with binding characteristics closely mirroring those of fluconazole. Importantly, our findings underscore the value of molecular modeling as a predictive tool in early-stage drug discovery, guiding rational design and prioritization of lead compounds for further biological evaluation. Collectively, the integration of these in silico results with experimental data significantly strengthens the scientific foundation of our study and supports the continued development of these novel antimicrobial agents.

**Table 2.** Active site residues for bacterial target protein penicillin binding protein, and fungal target protein P450 as specified by CB-DOCK 2 webserver.

Protein	Code in PDB	Chain	Active site Residues
Penicillin binding protein	3vsl	A	SER392 LYS395 ARG428 SER429 TYR430 HIS447 SER448 SER449
			ASN450 LYS600 ASP601 GLY602 THR603 GLY604 TYR605 VAL606
P450	5V5Z	A	SER607 LYS618 THR619 GLY620 THR621 ASN633 SER634 THR635
			TYR636 GLN656 VAL658 PRO660 LEU663 THR664 GLY665 GLY666)
			(PHE105 TYR118 LEU121 THR122 PHE126 ILE131 TYR132 LEU139
			MET140 GLN142 LYS143 ALA146 PHE228 LEU300 GLY303 ILE304
			GLY307 GLY308 THR311 SER312 LEU370 MET374 PRO375 LEU376
			ILE379 ARG381 PRO406 LEU461 PRO462 PHE463 GLY464 ARG467
			HIS468 ARG469 CYS470 ILE471 GLY472 GLU473 PHE475 ALA476
			GLN479 MET508)

**Table 3.** Ligand-protein interactions as analyzed from 2D interaction images obtained from discovery studio software.

Penicillin binding protein			
Ligand	Score of docking	Bonds	Interacting amino acids
<b>3a</b>	-6.4	- Hydrogen bond - alkyl bond - pi – alkyl bond	- SER 392 - TYR 430, PRO 660 - ILE 522
<b>Cefotaxime</b>	-7.9	- hydrogen bond -salt bridge bond - carbon-hydrogen bond	- SER 448, THR 621, THR 619, GLU 623, GLN 524 - GLU 623, LYS 618 -GLU 623, GLY 620, SER 392, THR 621
P450			
Ligand	Score of docking kcal/mol	Bonds	Interacting amino acids
<b>3c</b>	-7.8	- pi-cation - pi-anion - pi-alkyl - alkyl bond - carbon-hydrogen bond Pi donor hydrogen bond	- PHE 463 - PHE 463 - CYS 470, ALA 476 - LYS 143, ILE 471, ILE 131 -PRO 375 -CYS 470
<b>Fluconazole</b>	-8.9	-halogen bond -pi-alkyl - pi-sigma bond -pi-pi T Shaped bond -carbon-hydrogen bond	-GLY 303 -LEU 121, MET 508, LEU 376, ILE 131 -THR 311 -TYR 118 - GLY 307

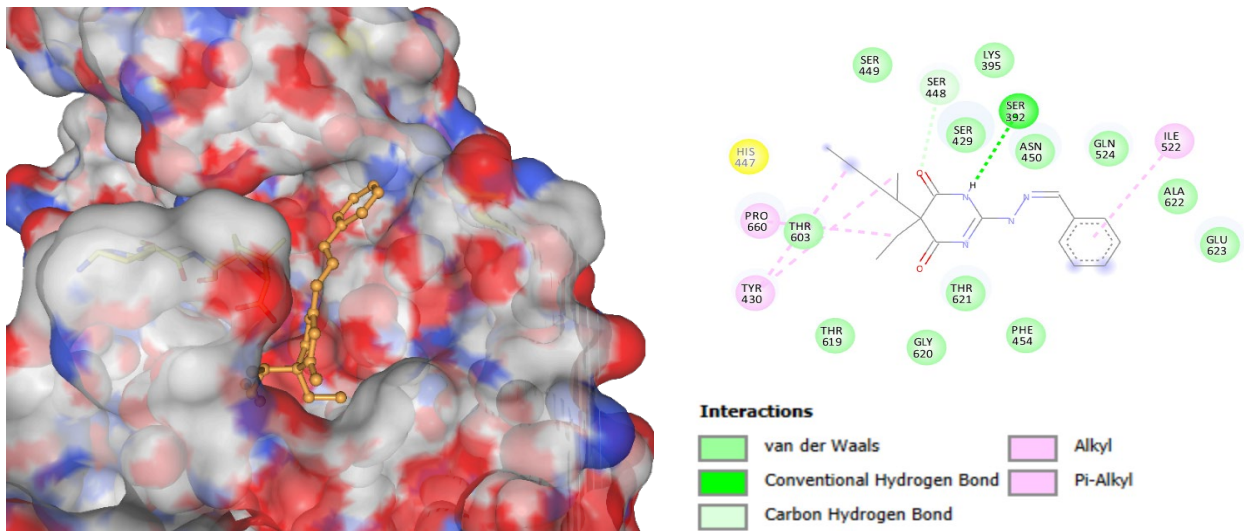


Fig. 2. Compound 3a on the active site of penicillin binding protein.

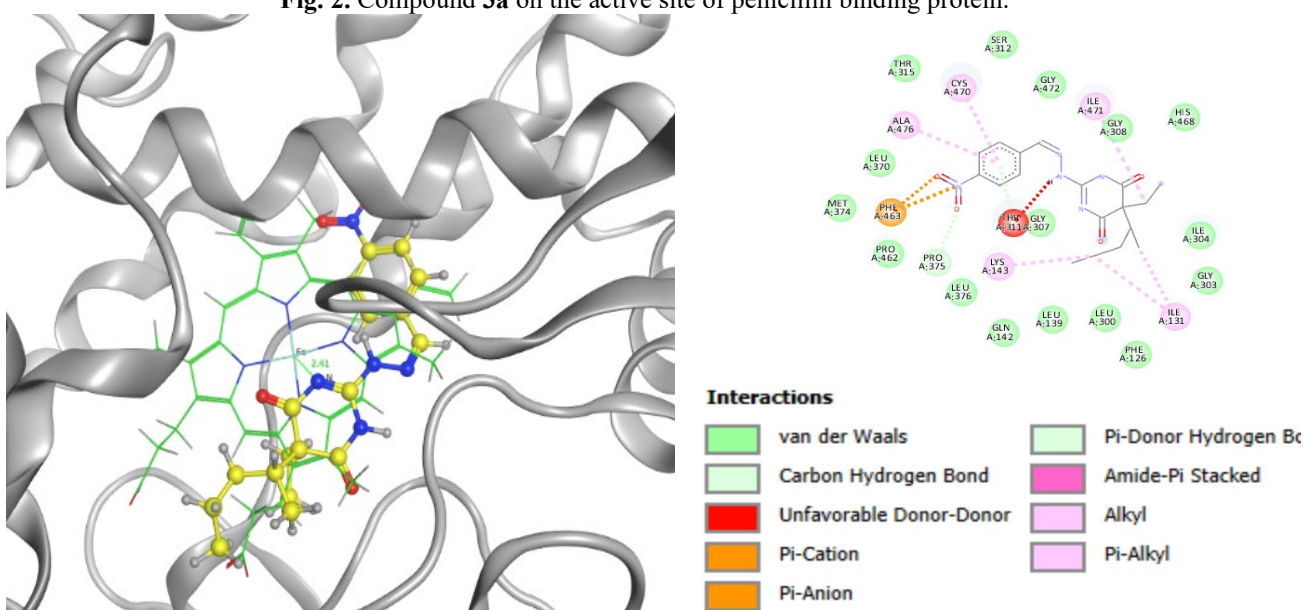


Fig. 3. Compound 3c on active site of fungal protein P450.

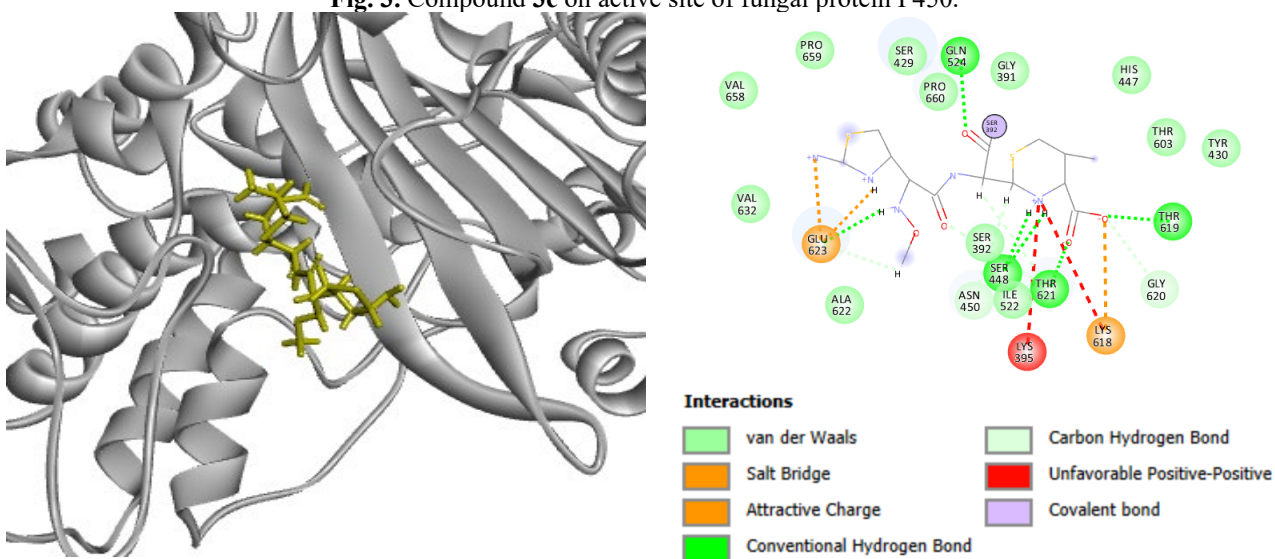


Fig. 4. Cefotaxime on active site of penicillin binding protein.

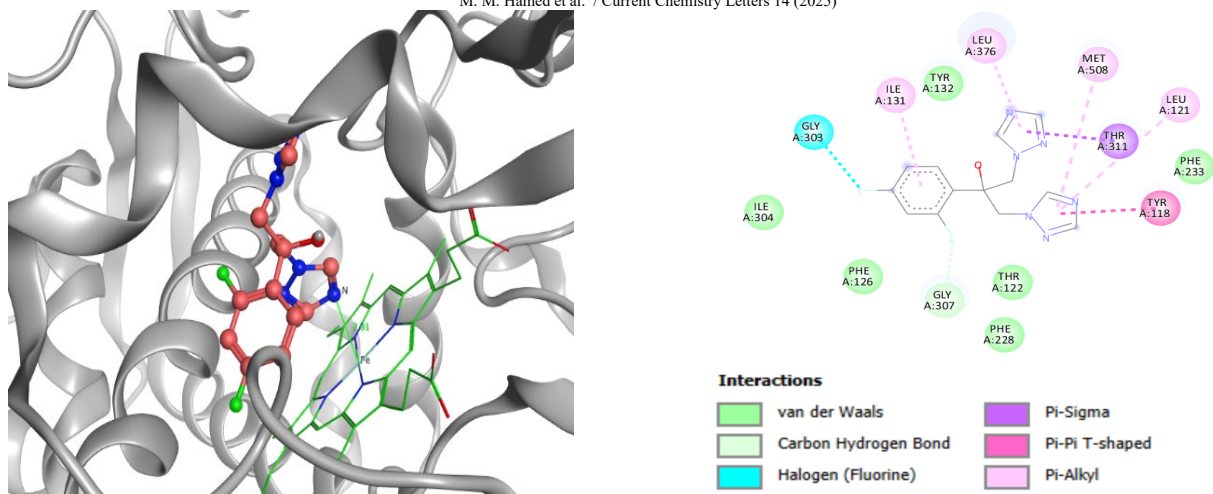


Fig. 5. Fluconazole on active site of P450.

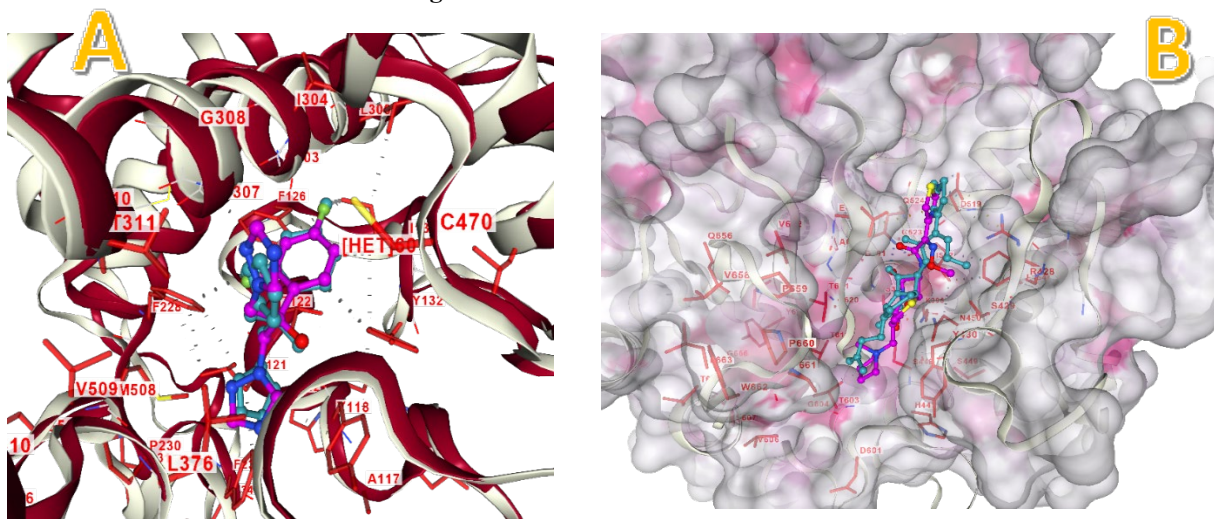


Fig. 6. Docking validation by docking back on cocrystal (A) fluconazole and (B) cefotaxime.

### 3. Experimental

#### 3.1. Chemistry

Melting points were determined on a GmbH-VarioEL V.3 micro-analyzer electro-thermal melting point apparatus and are uncorrected. FT-IR spectra were recorded as potassium bromide disks using Pye-Unicam Sp-100 infrared spectrophotometer.  $^1\text{H-NMR}$  and  $^{13}\text{C-NMR}$  spectra were carried on Jeol 400 MHz spectrometer. JEOL JMS-600 and Hewlett-Packard model MS 5988 Spectrometers were used for the determination of mass spectra. CHN microanalyses were conducted using a Perkin Elmer 2400 LS Series CHN/O Analyser. TLC was carried out on aluminium-backed silica gel plates (Merck 60F<sub>254</sub>) and visualized under short-wave UV light. Reactions performed at air atmosphere. The substance sodium thiopental (A), utilized for medical purposes, was sourced from (CHEMISCHE FABRIK BERG), and the corresponding certificate of analysis is included in the attached files.

#### Preparation of 5-ethyl-5-(pentan-2-yl)-2-thioxodihydropyrimidine-4,6(1*H*,5*H*)-dione (1)

(5g, 18.93 mmol) of sodium thiopental (A) was dissolved in (100 ml)  $\text{H}_2\text{O}$  then drops of HCL (30%) added drop wise with stirring, white ppt was formed, filtered off, drying, then recrystallization from (petroleum ether – ethanol) as white crystals; m.p 158-160 °C; yield 95 %; FT-IR (KBr)  $\text{cm}^{-1}$  showed bands at 3264, 3154 (2NH groups), 2959, 2933, and 2874 (C-H aliphatic), 1671, 1735 (2 C=O groups), 1543 (C-N);  $^1\text{H-NMR}$  (400 MHz,  $\text{DMSO-}d_6$ )  $\delta$  (ppm): 0.71 (t, 3H,  $\text{CH}_3$ ), 0.82 (t, 3H,  $\text{CH}_3$ ), 0.91 (d, 3H,  $\text{CH}_3$ ), 1.06 (q, 2H,  $\text{CH}_2$ ), 1.37 (m, 2H,  $\text{CH}_2$ ), 1.89 (q, 2H,  $\text{CH}_2$ ), 2.02 (m, 1H, CH), 12.61 (s, 2H, 2NH);  $^{13}\text{C-NMR}$  (100 MHz,  $\text{DMSO-}d_6$ )  $\delta$  (ppm): 0.91(C16), 9.50(C15), 12.49(C12), 19.89(C14), 27.19(C10), 32.23(C13), 41.23(C11), 58.96(C3), 169.96(C2), 170.25(C4), 178.62(C6). EI-MS: m/z 242.2,  $[\text{M}]^+$ . Anal. calcd. for  $\text{C}_{11}\text{H}_{18}\text{N}_2\text{O}_2\text{S}$  (242.34): C, 54.52; H, 7.49; N, 11.56; S, 13.23. Found: C, 54.57; H, 7.43; N, 11.63; S, 13.29%.

### 5-Ethyl-2-hydrazinyl-5-(pentan-2-yl)pyrimidine-4,6(1*H*,5*H*)-dione (2)

A mixture of thiopental compound (**1**) (2g, 8.26 mmol) in (20) ml absolute ethanol, hydrazine hydrate (0.63 ml, 20 mmol) was added, the mixture was refluxed for 8 h. cooling, then poured the mixture into ice bath, the solid product was filtered off, dried and recrystallized from ethanol as white crystals; m.p 193-195 °C; yield 67 %; FT-IR (KBr)  $\text{cm}^{-1}$  showed bands at 3344 (NH<sub>2</sub> group), 3234 (2NH groups), 2960, 2933, and 2874 (C-H aliphatic), 1687, 1713 (2 C=O groups), 1638 (C-N); <sup>1</sup>H-NMR (400 MHz, DMSO-*d*<sub>6</sub>)  $\delta$  (ppm): 0.68 (t, 3H, CH<sub>3</sub>), 0.82 (t, 3H, CH<sub>3</sub>), 0.90 (d, 3H, CH<sub>3</sub>), 1.06 (q, 2H, CH<sub>2</sub>), 1.36 (m, 2H, CH<sub>2</sub>), 1.83 (q, 2H, CH<sub>2</sub>), 1.91 (m, 1H, CH), 7.76 (s, 4H, 2NH, 1NH<sub>2</sub>); <sup>13</sup>C-NMR (100 MHz, DMSO-*d*<sub>6</sub>)  $\delta$  (ppm): 9.90(C15), 14.27(C14), 14.94(C11), 20.96(C13), 27.29(C9), 33.60(C12), 41.30(C10), 42.36(C3), 60.05(C6), 172.00(C2), 172.69(C4). EI-MS: m/z 240.4, [M]<sup>+</sup>. Anal. calcd. for C<sub>11</sub>H<sub>20</sub>N<sub>4</sub>O<sub>2</sub> (240.31): C, 54.98; H, 8.39; N, 23.32. Found: C, 54.91; H, 8.33; N, 23.37%.

### Synthesis of some schiff base derivatives from 5-ethyl-2-hydrazinyl-5-(pentan-2-yl)pyrimidine-4,6(1*H*,5*H*)-dione (3 a-c).

#### General procedure:

A mixture of compound **2** (1g, 4.16 mmol) and aromatic aldehyde (4.16 mmol) in (20) ml absolute ethanol in presence of few drops of piperidine was heated under reflux for 5 hr. The solid product which obtained after cooling was filtered off, dried and recrystallized from proper solvent.

### 2-(2-Benzylidenehydrazinyl)-5-ethyl-5-(pentan-2-yl)pyrimidine-4,6(1*H*,5*H*)-dione (3a)

The solid thus formed by the reaction with benzaldehyde, recrystallized from ethanol to afford white crystals; m.p 170-172 °C; yield 79 %; FT-IR (KBr)  $\text{cm}^{-1}$  showed bands at 3269, 3152 (2NH groups), 3044 (C-H aromatic), 2957, 2933, and 2873 (C-H aliphatic), 1671, 1735 (2C=O groups), 1543 (C-N); <sup>1</sup>H-NMR (400 MHz, DMSO-*d*<sub>6</sub>)  $\delta$  (ppm): 0.75 (t, 3H, CH<sub>3</sub>), 0.83 (t, 3H, CH<sub>3</sub>), 0.97 (d, 3H, CH<sub>3</sub>), 1.11 (q, 2H, CH<sub>2</sub>), 1.40 (m, 2H, CH<sub>2</sub>), 1.92 (q, 2H, CH<sub>2</sub>), 2.01 (m, 1H, CH), 7.00-8.20 (m, 5H, Ar-H), 8.34 (s, 1H, CH), 11.35 (s, 2H, 2NH); <sup>13</sup>C-NMR (100 MHz, DMSO-*d*<sub>6</sub>)  $\delta$  (ppm): 0.21(C15), 8.82(C14), 13.17(C11), 19.22(C13), 26.22(C9), 32.91(C12), 41.27(C10), 59.26(C3), 127.49(C20), 127.86(C21), 128.17(C20, C24:Ph), 128.85(C21, C23:Ph), 129.83(C22:Ph), 134.20(C19), 146.24(C18), 155.57(C6), 169.65(C2), 170.93(C4). EI-MS: m/z 328.3, [M]<sup>+</sup>. Anal. calcd. for C<sub>18</sub>H<sub>24</sub>N<sub>4</sub>O<sub>2</sub> (328.42): C, 65.83; H, 7.37; N, 17.06. Found: C, 65.94; H, 7.32; N, 17.01%.

### 2-(2-(4-Chlorobenzylidene)hydrazinyl)-5-ethyl-5-(pentan-2-yl)pyrimidine-4,6(1*H*,5*H*)-dione (3b)

Obtained by the reaction with *p*-chloro benzaldehyde and recrystallized from ethanol as white crystals; m.p 188-190 °C; yield 75 %; FT-IR (KBr)  $\text{cm}^{-1}$  showed bands at 3181 (2NH groups), 3043 (C-H aromatic), 2959, 2873 (C-H aliphatic), 1645, 1703 (2C=O groups), 1616 (C-N); <sup>1</sup>H-NMR (400 MHz, DMSO-*d*<sub>6</sub>)  $\delta$  (ppm): 0.75 (t, 3H, CH<sub>3</sub>), 0.83 (t, 3H, CH<sub>3</sub>), 0.96 (d, 3H, CH<sub>3</sub>), 1.08 (q, 2H, CH<sub>2</sub>), 1.40 (m, 2H, CH<sub>2</sub>), 1.92 (q, 2H, CH<sub>2</sub>), 2.01 (m, 1H, CH), 7.00-8.20 (m, 4H, Ar-H), 8.34 (s, 1H, CH), 11.46 (s, 2H, 2NH); <sup>13</sup>C-NMR (100 MHz, DMSO-*d*<sub>6</sub>)  $\delta$  (ppm): 0.18(C15), 9.90(C14), 14.26(C11), 20.59(C13), 27.97(C9), 33.61(C12), 42.34(C10), 60.35(C3), 128.26(C20:Ph), 128.93(C24:Ph), 129.93(C21:Ph), 130.68(C23:Ph), 133.62(C19), 135.57(C22), 147.32(C18), 155.30(C6), 170.73(C2), 172.02(C4). EI-MS: m/z 362.3, [M]<sup>+</sup>. Anal. calcd. for C<sub>18</sub>H<sub>23</sub>ClN<sub>4</sub>O<sub>2</sub> (362.86): C, 59.58; H, 6.39; N, 15.44. Found: C, 59.52; H, 6.43; N, 15.40%.

### 5-Ethyl-2-(2-(4-nitrobenzylidene)hydrazinyl)-5-(pentan-2-yl)pyrimidine-4,6(1*H*,5*H*)-dione (3c)

It was obtained from **2** and *p*-nitro benzaldehyde as above procedure then recrystallized from ethanol as yellow crystals; m.p 160-161 °C; yield 83 %; FT-IR (KBr)  $\text{cm}^{-1}$  showed bands at 3242, 3153 (2NH groups), 3066 (C-H aromatic), 2958, 2931, and 2873 (C-H aliphatic), 1646, 1712 (2 C=O groups), 1593 (C-N); <sup>1</sup>H-NMR (400 MHz, DMSO-*d*<sub>6</sub>)  $\delta$  (ppm): 0.75 (t, 3H, CH<sub>3</sub>), 0.83 (t, 3H, CH<sub>3</sub>), 0.97 (d, 3H, CH<sub>3</sub>), 1.09 (q, 2H, CH<sub>2</sub>), 1.40 (m, 2H, CH<sub>2</sub>), 1.94 (q, 2H, CH<sub>2</sub>), 2.00 (m, 1H, CH), 8.00-8.40 (m, 4H, Ar-H), 8.47 (s, 1H, CH), 11.49 (s, 2H, 2NH); <sup>13</sup>C-NMR (100 MHz, DMSO-*d*<sub>6</sub>)  $\delta$  (ppm): 0.21(C15), 9.14(C14), 13.51(C11), 19.89(C13), 26.22(C9), 32.55(C12), 41.28(C10), 59.96(C3), 123.13(C20:Ph), 123.82(C24:Ph), 124.19(C21:Ph), 124.49(C23:Ph), 128.82(C19), 140.53(C18), 147.60(C22), 152.96(C6), 169.66(C2), 170.91(C4). EI-MS: m/z 373.3, [M]<sup>+</sup>. Anal. calcd. for C<sub>18</sub>H<sub>23</sub>N<sub>5</sub>O<sub>4</sub> (373.41): C, 57.90; H, 6.21; N, 18.76. Found: C, 57.95; H, 6.22; N, 18.71%.

### 2-(2-(5-Chloro-3-oxoindolin-2-ylidene)hydrazinyl)-5-ethyl-5-(pentan-2-yl)pyrimidine-4,6(1*H*,5*H*)-dione (4)

A sample of compound **2** (1g, 4.16 mmol) and 5 chloro isatin (0.75 g, 4.16 mmol) in (20) ml absolute ethanol in the presence of drops of piperidine were refluxed for 5 hr., and then the reaction mixture was allowed to cool. The solid precipitate formed was filtered off, dried and recrystallized from ethanol as brown crystals; m.p over 300 °C; yield 77 %; FT-IR (KBr)  $\text{cm}^{-1}$  showed bands at 3351, 3149 (3NH groups), 3071 (C-H aromatic), 2959, 2931, 2873, and 2839 (C-H aliphatic), 1666, 1691, and 1718 (3C=O groups), 1607 (C-N); <sup>1</sup>H-NMR (400 MHz, DMSO-*d*<sub>6</sub>)  $\delta$  (ppm): 0.77 (t, 3H, CH<sub>3</sub>), 0.83 (t, 3H, CH<sub>3</sub>), 0.96 (d, 3H, CH<sub>3</sub>), 1.11 (q, 2H, CH<sub>2</sub>), 1.41 (m, 2H, CH<sub>2</sub>), 1.96 (q, 2H, CH<sub>2</sub>), 2.05 (m, 1H, CH), 6.50-7.50 (m, 3H, Ar-H), 8.51 (s, 1H, NH), 10.85 (s, 1H, NH), 12.37 (s, 1H, NH); <sup>13</sup>C-NMR (100 MHz, DMSO-*d*<sub>6</sub>)  $\delta$  (ppm): 0.57(C16), 9.91(C15), 14.26(C12), 20.59(C14), 27.60(C10), 34.29(C13), 42.66(C11), 61.39(C3), 112.22(C22), 118.25 (C25),

126.90(C20), 127.89(C24), 131.57(C23), 142.64(C21), 146.27(C19), 151.68 (C6), 165.38 (C17), 170.36 (C2), 172.69(C4). Anal. calcd. for C<sub>19</sub>H<sub>22</sub>ClN<sub>5</sub>O<sub>3</sub> (403.87): C, 56.51; H, 5.49; N, 17.34. Found: C, 56.53; H, 5.42; N, 17.39%.

### 3.2. Docking studies

In docking studies we focused on our compounds **3a** and **3c**, we have used CB-DOCK 2 webserver to perform molecular docking of compound **3a** against bacterial target protein which is called penicillin binding protein which was resolved by X-RAY DIFFRACTION in Resolution of 2.40 Å containing crystal ligand cefotaxime, and compound **3c** against the well-recognized fungal target protein CYP51 from the pathogen *Candida albicans* which also was resolved with X-RAY DIFFRACTION in Resolution of 2.90 Å containing a heme group in the active site with its central attached iron atom, both protein structures were obtained from protein data bank and saved as PDB files, active sites for each protein was specified using site finder tool built in CB-DOCK 2 as shown in **Table (1)**, we used discovery studio software to generate the **2d** illustrations of complexes interactions. Cefotaxime was used as a positive control against bacteria and fluconazole as a positive control against fungi, both were downloaded from PubChem database in SDF format, and before docking of our compounds we performed a docking validation to confirm reliability of our docking protocol. Both of our compounds **3a** and **3c** were drawn using chemdraw software and saved as SDF files for further use in docking as ligands.

### 4. Conclusion

This study successfully designed and synthesized a novel series of thiopental-based alkylpyrimidine derivatives (**3a-c**, **4**) through efficient condensation reactions, characterized using spectroscopic techniques (FT-IR, NMR, and mass spectrometry). The antimicrobial evaluation revealed promising activity, with **3a** selectively inhibiting *Bacillus subtilis* (MIC: 10.5±0.4 mg/mL) and *Escherichia coli* (MIC: 22.1±0.3 mg/mL), while **3c** exhibited potent antifungal effects against *Candida albicans* (MIC: 11.6±0.4 mg/mL). Molecular docking studies provided mechanistic insights, demonstrating that **3a** binds to penicillin-binding protein (PBP; -6.4 kcal/mol) via hydrogen bonds and hydrophobic interactions, while **3c** targets fungal CYP51 (-7.8 kcal/mol) through heme iron coordination and  $\pi$ -cation/anion interactions, mimicking fluconazole's mode of action. The structure-activity relationship (SAR) analysis highlighted the critical role of electron-deficient pyrimidine cores for antibacterial activity and thioether moieties for antifungal specificity. Despite **3a**'s narrower spectrum compared to cefotaxime, and **3c**'s lower affinity than fluconazole, these derivatives offer scaffold versatility for further optimization. Integration of synthetic, biological, and computational approaches validated their potential as dual-target antimicrobial agents. Future work will focus on structural modifications to enhance binding affinity, broaden spectrum activity, and evaluate pharmacokinetic properties. This study underscores the promise of thiopental-pyrimidine hybrids in addressing antimicrobial resistance and paves the way for their development as next-generation therapeutics.

### Conflicts of interest

There are no conflicts of interest to be declared.

### References

- [1] Koubi Y., Moukhliiss Y., Hajji H., Abdessadak O., Alaqarbeh M., Ajana M. A., Maghat H., Lakhlifi T., and Bouachrine M. (2024) Computational structure–biological activity and retrosynthesis investigations of 1,2,3-triazole-quinoline hybrid molecules as potential respiratory virus inhibitors. *Chem. Heterocycl. Compd.*, 60 (9/10) 491-504.
- [2] Wei J., Chen L., Zhu K., Cheng Y. X., and Huang D. (2024) Design, synthesis, and fungicidal activity evaluation of 2-methyl-5-phenylthiazole-4-carboxamides bearing morpholine, thiomorpholine, or thiomorpholine 1,1-dioxide moiety. *Chem. Heterocycl. Compd.*, 60 (9/10) 536-543.
- [3] Molchanova M. V., Ikonnikova V. A., Anisenko A. N., Gottikh M. B., Baranov M. S., and Mikhaylov A. A. (2024) The cycloaddition reaction of benzothiazolium ylides with  $\alpha$ -cyanocinnamamides: the synthesis of structural analogs of inhibitors of HIV-1 post-integrational repair. *Chem. Heterocycl. Compd.*, 60 (9/10) 544-548.
- [4] Mohamed S. K., Mague J. T., Akkurt M., Alfayomy A. M., Abou Seri S. M., Abdel-Raheem Sh. A. A., and Abdul-Malik M. A. (2022) Crystal structure and Hirshfeld surface analysis of ethyl (3*E*)-5-(4-chlorophenyl)-3-[[4-chlorophenyl]formamido]imino}-7-methyl-2*H*,3*H*,5*H*-[1,3]thiazolo[3,2-*a*]pyrimidine-6-carboxylate. *Acta Cryst.*, 78 (8) 846-850.
- [5] Abdel-Raheem Sh. A. A., Drar A. M., Hussein B. R. M., and Moustafa A. H. (2023) Some oxoimidazolidine and cyanoguanidine compounds: Toxicological efficacy and structure-activity relationships studies. *Curr. Chem. Lett.*, 12 (4) 695–704.
- [6] El Bakri Y., Mohamed S. K., Saravanan K., Ahmad S., Mahmoud A. A., Abdel-Raheem Sh. A. A., ElSayed W. M., Mague J. T., and Said S. G. (2023) 1,4,9,9-tetramethyloctahydro-4,7-(epoxymethano)azulen-5(1*H*)-one, a natural product as a potential inhibitor of COVID-19: Extraction, crystal structure, and virtual screening approach. *J. King Saud Univ. Sci.*, 35 (4) 102628.
- [7] Abdelhamid A. A., Elsaghier A. M. M., Aref S. A., Gad M. A., Ahmed N. A., and Abdel-Raheem Sh. A. A. (2021) Preparation and biological activity evaluation of some benzoylthiourea and benzoylurea compounds. *Curr. Chem. Lett.*, 10 (4) 371-376.

- [8] Fouad M. R., Shamsan A. Q. S., and Abdel-Raheem Sh. A. A. (2023) Toxicity of atrazine and metribuzin herbicides on earthworms (*Aporrectodea caliginosa*) by filter paper contact and soil mixing techniques. *Curr. Chem. Lett.*, 12 (1) 185–192.
- [9] Fouad M. R., and Abdel-Raheem Sh. A. A. (2024) An overview on the fate and behavior of imidacloprid in agricultural environments. *Environ. Sci. Pollut. Res.*, 31 61345-61355.
- [10] Ibrahim S. M., Abdelkhalek A. S., Abdel-Raheem Sh. A. A., Freaah N. E., El Hady N. H., Aidia N. K., Tawfeq N. A., Gomaa N. I., Fouad N. M., Salem H. A., Ibrahim H. M., and Sebaiy M. M. (2024) An overview on 2-indolinone derivatives as anticancer agents. *Curr. Chem. Lett.*, 13 (1) 241-254.
- [11] Mohamed S. K.; Mague J. T.; Akkurt M.; Alfayomy A. M.; Ragab F. A., and Abd ul-Malik M. A. (2022) Crystal structure and Hirshfeld surface analysis of ethyl (3E)-5-(4-fluorophenyl)3-[[4-methoxyphenyl]formamido]imino}-7-methyl-2H,3H,5H-[1,3]thiazolo[3,2-a]pyrimidine-6-carboxylate 0.25-hydrate. *Acta Cryst.*, 78 (9) 880-884.
- [12] Abd ul-Malik M. A.; Kamal El-Dean A. M.; Radwan S. M.; and Zaki R. M. (2021) Facile synthesis and antimicrobial evaluations of some novel pyrazolo[3,4-b]selenolo[3,2-e]pyrazines and their related heterocycles. *J. Heterocycl. Chem.*, 58 (11) 2067-2077.
- [13] Zaki R. M., Kamal El-Dean A. M., Radwan S. M., and Abdul-Malik M. A. (2020) Efficient synthesis, reactions, and biological activities of new thieno and furopyrazolo[3,4-b]pyrazines and their related heterocycles. *J. Chin. Chem. Soc.*, 67 (4) 658-673.
- [14] Alshera`a A. A., Hussein A. M., Kamal El-Dean A. M., Thabet E. A., Abdul-Malik M. A., Gad M. A., Qaid F. M. Q., Abdelkhalek A. S., and Abdel-Raheem Sh. A. A. (2025) Chemical design, preparation, agricultural bioefficacy valuation, and molecular docking of some pyridine containing compounds, *Curr. Chem. Lett.*, 14 (3) 407-416.
- [15] Abd-Ella A. A., Metwally S. A., Abdul-Malik M. A., El-Ossaily Y. A., AbdElrazek F. M., Aref S. A., Naffea Y. A., and Abdel-Raheem Sh. A. A. (2022) A review on recent advances for the synthesis of bioactive pyrazolinone and pyrazolidinedione derivatives. *Curr. Chem. Lett.*, 11 (2) 157-172.
- [16] Sebaiy M. M., El-Adl S. M., Nafea A., Mattar A. A., Abdul-Malik M. A., Abdel-Raheem Sh. A. A., and Elbaramawi S. S. (2024) Review: Instrumental Analytical techniques for Evaluating some Anti-infective Drugs in Pharmaceutical Products and Biological Fluids. *Curr. Chem. Lett.*, 13 491-502.
- [17] Abdelkhalek A. S., Abokull M. E., Ibrahim S. M., Soltan M. K., Abdul-Malik M. A., and Abdel-Raheem Sh. A. A. (2024) A review on some synthetic methods of 4(3H)-quinazolinone and benzotriazepine derivatives and their biological activities. *Org. Commun.*, 17 63–98.
- [18] Sebaiy M. M., El-Adl S. M., Elbaramawi S. S., Abdel-Raheem Sh. A. A., and Nafie A. (2024) Developing a highly validated and sensitive HPLC method for simultaneous estimation of cefotaxime and paracetamol in pure and pharmaceutical preparations. *Curr. Chem. Lett.*, 13 435-444.
- [19] El-Ossaily Y. A., Alanazi N. M. M., Althobaiti I. O., Altaieb H. A., Al-Muailkel N. S., El-Sayed M. Y., Hussein M. F., Ahmed I. M., Alanazi M. M., Fawzy A., Abdel-Raheem Sh. A. A., and Tolba M. S. (2024) Multicomponent Approach to the Synthesis and Spectral Characterization of Some 3,5-Pyrazolididione Derivatives and Evaluation as Anti-inflammatory Agents. *Curr. Chem. Lett.*, 13 (1) 127-140.
- [20] Abdul-Malik M. A., Abdou A., Fouad M. R., Alkamali A. S. N., and Abdel-Raheem Sh. A. A. (2024) Synthesis, spectral characterization and molecular docking studies of some thiocarbohydrazide-based Schiff bases with pyrazole moiety as potential anti-inflammatory agents. *Curr. Chem. Lett.*, 13 683–694.
- [21] Gad M. A., Aref S. A., Abdelhamid A. A., Elwassimy M. M., and Abdel-Raheem Sh. A. A. (2021) Biologically active organic compounds as insect growth regulators (IGRs): introduction, mode of action, and some synthetic methods. *Curr. Chem. Lett.*, 10 (4) 393-412.
- [22] Elhady O. M., Mansour E. S., Elwassimy M. M., Zawam S. A., Drar A. M., and Abdel-Raheem Sh. A. A. (2022) Selective synthesis, characterization, and toxicological activity screening of some furan compounds as pesticidal agents. *Curr. Chem. Lett.*, 11 (3) 285-290.
- [23] Hussein B. R. M., Moustafa A. H., Abdou A.; Drar A. M., and Abdel-Raheem Sh. A. A. (2024) Preparation, agricultural bioactivity evaluation, structure-activity relationships estimation, and molecular docking of some quinazoline compounds. *J. Agric. Food Chem.*, 72 8973–8982.
- [24] Abdel-Raheem Sh. A. A., Kamal El-Dean A. M., Zaki R. M., Hassanien R., El-Sayed M. E. A., Sayed M., and Abd-Ella A. A. (2021) Synthesis and toxicological studies on distyryl-substituted heterocyclic insecticides. *Eur. Chem. Bull.*, 10 (4) 225-229.
- [25] Abdel-Raheem Sh. A. A., Kamal El-Dean A. M., Abdul-Malik M. A., Hassanien R., El-Sayed M. E. A., Abd-Ella A. A., Zawam S. A., and Tolba M. S. (2022) Synthesis of new distyrylpyridine analogues bearing amide substructure as effective insecticidal agents. *Curr. Chem. Lett.*, 11 (1) 23-28.
- [26] Tolba M. S., Abdul-Malik M. A., Kamal El-Dean A. M., Geies A. A., Radwan Sh. M., Zaki R. M., Sayed M., Mohamed S. K., and Abdel-Raheem Sh. A. A. (2022) An overview on synthesis and reactions of coumarin based compounds. *Curr. Chem. Lett.*, 11 (1) 29-42.
- [27] Abdel-Raheem Sh. A. A., Kamal El-Dean A. M., Hassanien R., El-Sayed M. E. A., and Abd-Ella A. A. (2021) Synthesis and characterization of some distyryl-derivatives for agricultural uses. *Eur. Chem. Bull.*, 10 (1) 35-38.

- [28] Kamal El-Dean A. M., Abd-Ella A. A., Hassanien R., El-Sayed M. E. A., and Abdel-Raheem Sh. A. A. (2019) Design, Synthesis, Characterization, and Insecticidal Bioefficacy Screening of Some New Pyridine Derivatives. *ACS Omega*, 4 (5) 8406-8412.
- [29] Abdel-Raheem Sh. A. A., Kamal El-Dean A. M., Hassanien R., El-Sayed M. E. A., Sayed M., and Abd-Ella A. A. (2021) Synthesis and spectral characterization of selective pyridine compounds as bioactive agents. *Curr. Chem. Lett.*, 10 (3) 255-260.
- [30] Kamal El-Dean A. M., Abd-Ella A. A., Hassanien R., El-Sayed M. E. A., Zaki R. M., and Abdel-Raheem Sh. A. A. (2019) Chemical design and toxicity evaluation of new pyrimidothienotetrahydroisoquinolines as potential insecticidal agents. *Toxicol. Rep.*, 6 (2019) 100-104.
- [31] Abdul-Malik M. A., Zaki R. M., Kamal El-Dean A. M., and Radwan S. M. A (2018) concise review on the synthesis and reactions of pyrazolopyrazine heterocycles. *J. Heterocycl. Chem.*, 55 (8) 1828-1853.
- [32] Zaki R. M., El-Dean A. M., Radwan S. M., Abdul-Malik M. A. (2018) A facile synthesis, reactions, and spectral characterization of some novel thieno[3,2-*e*]pyrazolo[3,4-*b*]pyrazine compounds. *J. Chin. Chem. Soc.*, 65 (11) 1407-1414.
- [33] Kamal El-Dean A. M.; Radwan S. M.; Zaki R. M.; and Abd ul-Malik M. A. (2018) Efficient synthesis of some novel furo[3,2-*e*]pyrazolo[3,4-*b*]pyrazines and related heterocycles. *Synth. Commun.*, 48 (4) 395-412.
- [34] Abdel-Raheem Sh. A. A., Kamal El-Dean A. M., Abdul-Malik M. A., Marae I. S., Bakhite E. A., Hassanien R., El-Sayed M. E. A., Zaki R. M., Tolba M. S., Sayed A. S. A., and Abd-Ella A. A. (2022) Facile synthesis and pesticidal activity of substituted heterocyclic pyridine compounds. *Rev. Roum. Chem.*, 67 (4-5) 305-309.
- [35] Abdelkhalek A. S., Abdulrahman A., Abokull M. E., Ibrahim S. M., Soltan M. K., Abdul-Malik M. A., and Abdel-Raheem Sh. A. A. (2025) An overview of pyrazolo[3,4-*d*]pyrimidine heterocycles: recent synthetic approaches and biological activities. *J. Indian Chem. Soc.*, 102 (7) 101763.
- [36] Tolba M. S., Kamal El-Dean A. M., Ahmed M., Hassanien R., Sayed M., Zaki R. M., Mohamed S. K., Zawam S. A., and Abdel-Raheem Sh. A. A. (2022) Synthesis, reactions, and applications of pyrimidine derivatives. *Curr. Chem. Lett.*, 11 (1) 121-138.
- [37] Tolba M. S., Sayed M., Abdel-Raheem Sh. A. A., Gaber T. A., Kamal El-Dean A. M., and Ahmed M. (2021) Synthesis and spectral characterization of some new thiazolopyrimidine derivatives. *Curr. Chem. Lett.*, 10 (4) 471-478.
- [38] Drar A. M., Abdel-Raheem Sh. A. A., Moustafa A. H., and Hussein B. R. M. (2023) Studying the toxicity and structure-activity relationships of some synthesized polyfunctionalized pyrimidine compounds as potential insecticides. *Curr. Chem. Lett.*, 12 (3) 499-508.
- [39] Tolba M. S., Sayed M., Kamal El-Dean A. M., Hassanien R., Abdel-Raheem Sh. A. A., and Ahmed M. (2021) Design, synthesis and antimicrobial screening of some new thienopyrimidines. *Org. Commun.*, 14 (4) 365-376.
- [40] Manna T., Maji S., Maity M., Debnath B., Panda S., Khan S. A., Nath R., and Akhtar M. J. (2025) Anticancer potential and structure activity studies of purine and pyrimidine derivatives: an updated review. *Mol. Divers.*, 29 (1) 817-848.
- [41] Lagoja I. M. (2005) Pyrimidine as constituent of natural biologically active compounds. *Chem. Biodivers.*, 2 (1) 1-50.
- [42] Bushby S. R., and Hitchings G. H. (1968) Trimethoprim, a sulphonamide potentiator. *Br. J. Pharmac. Chemother.*, 33 (1) 72-90.
- [43] Capdeville R., Buchdunger E., Zimmermann J., and Matter A. (2002) Glivec (STI571, imatinib), a rationally developed, targeted anticancer drug. *Nat. Rev. Drug Discov.*, 1 (7) 493-502.
- [44] Elkhalfifa D., Siddique A. B., Qusa M., Cyprian F. S., El Sayed K., Alali F., Al Moustafa A., and Khalil A. (2020) Design, synthesis, and validation of novel nitrogen-based chalcone analogs against triple negative breast cancer. *Eur. J. Med. Chem.*, 187 111954.
- [45] Kumar G., and Singh N. P. (2021) Synthesis, anti-inflammatory and analgesic evaluation of thiazole/oxazole substituted benzothiazole derivatives. *Bioorg. Chem.*, 107 104608.
- [46] Jiang X., Yu J., Zhou Z., Kongsted J., Song Y., Pannecouque C., Clercq E. D., Kang D., Poongavanam V., Liu X., and Zhan P. (2019) Molecular design opportunities presented by solvent-exposed regions of target proteins. *Med. Res. Rev.*, 39 (6) 2194-2238.
- [47] Rashid S., Yoshigoe Y., and Saito S. (2022) Phenanthroline based rotaxanes: recent developments in syntheses and applications. *RSC Adv.*, 12 (18) 11318-11344.
- [48] Scott M., and McCluggage W. G. (2003) Ovarian Cancer: Jacobs IJ, Shepherd JH, Oram DH, et al, eds.(£ 125.00.) Oxford University Press, 2002. ISBN 0 19850826 3.
- [49] Jeschke P. (2017) Latest generation of halogen-containing pesticides. *Pest Manag. Sci.*, 73 (6) 1053-1066.
- [50] Abdel-Raheem Sh. A. A., Fouad M. R., Gad M. A., Kamal El-Dean A. M., and Tolba M. S. (2023) Environmentally Green Synthesis and Characterization of Some Novel Bioactive Pyrimidines with Excellent Bioefficacy and Safety Profile Towards Soil Organisms. *J. Environ. Chem. Eng.*, 11 (5) 110839.
- [51] Wong W. Y., and Ho C. L. (2009) Heavy metal organometallic electrophosphors derived from multi-component chromophores. *Coord. Chem. Rev.*, 253 (13-14) 1709-1758.
- [52] Franks N. P., and Lieb W. R. (1994) Molecular and cellular mechanisms of general anaesthesia. *Nature*, 367 (6464) 607-614.

- [53] Osterblad M., Leistevuo J., Leistevuo T., Järvinen H., Pyy L., Tenovuo J., and Huovinen P. (1995) Antimicrobial and mercury resistance in aerobic gram-negative bacilli in fecal flora among persons with and without dental amalgam fillings. *Antimicrob. Agents Chemother.*, 39 (11) 2499-2502.
- [54] Alberti M. O., Hindler J. A., and Humphries R. M. (2016) Erratum for Alberti et al., Antimicrobial Susceptibilities of *Abiotrophia defectiva*, *Granulicatella adiacens*, and *Granulicatella elegans*. *Antimicrob. Agents Chemother.*, 60 (6) 3868-3868.
- [55] Sayiprathap B. R., Patibanda A. K., Prasanna Kumari V., Jayalalitha K., Ramappa H. K., Rajeswari E., Karthiba L., Saratbabu K., Sharma M., and Sudini H. K. (2022) Salient findings on host range, resistance screening, and molecular studies on sterility mosaic disease of pigeonpea induced by Pigeonpea sterility mosaic viruses (*PPSMV-I* and *PPSMV-II*). *Front. Microbiol.*, 13 838047.
- [56] Volkova T. V., and Perlovich G. L. (2020) Comparative analysis of solubilization and complexation characteristics for new antifungal compound with cyclodextrins. Impact of cyclodextrins on distribution process. *Eur. J. Pharm. Sci.*, 154 105531.
- [57] Fair R. J., and Tor Y. (2014) Antibiotics and bacterial resistance in the 21st century. *Perspect. Med. Chem.*, 6 25-64.
- [58] Tolba M. S., Ahmed M., Mohammed A. A., Saddik A. A., Sayed M., Hassanien R., Kamal El-Dean A. M., Hassan A., and Younis O. (2025) Synthesis, photoluminescence, antimicrobial evaluation, molecular docking, and pharmacokinetic prediction of new pyrimidoselenolo[2,3-*d*]pyrimidine derivatives. *J. Mol. Struct.*, 1336 142097.
- [59] Ahmed M., Hamed M. M., Sayed M., El-Rashedy A. A., El-Dean A. M. K., Hassan M. H., Mady M. F., and Tolba M. S. (2025) Synthesis, antimicrobial activity, molecular docking and molecular dynamics studies of novel bioactive compounds derived from propylthiouracil. *J. Mol. Struct.*, 1333 141779.
- [60] Hamed M. M., Ahmed M., Kamal El-Dean A. M., Hassan M. H., and Tolba M. S. (2025) Propylthiouracil Derivatives: Synthesis and Evaluation of Antimicrobial Efficacy Against Pathogenic Strains. *New Valley University Journal of Basic and Applied Sciences (NUJBAS)*, 3 (1) 1-9.
- [61] Ahadi S., Abaszadeh M., Khavasi H. R., and Bazgir A. (2012) An efficient three-component synthesis of new barbiturate salts. *Tetrahedron*, 68 (13) 2906-2916.
- [62] Alsedfy M. Y., Ebnalwaled A. A., Moustafa M., and Said A. H. (2024) Investigating the binding affinity, molecular dynamics, and ADMET properties of curcumin-IONPs as a mucoadhesive bioavailable oral treatment for iron deficiency anemia. *Sci. Rep.*, 14 (1) 22027.
- [63] Shivanika C., Kumar D., Rangunathan V., Tiwari P., and Sumitha A. (2020) Molecular docking, validation, dynamics simulations, and pharmacokinetic prediction of natural compounds against the SARS-CoV-2 main-protease. *J. Biomol. Struct. Dyn.*, 40 (2) 585-611.
- [64] Bertonha A. F., Silva C. C., Shirakawa K. T., Trindade D. M., and Dessen A. (2023) Penicillin-binding protein (PBP) inhibitor development: A 10-year chemical perspective. *Exp. Biol. Med.*, 248 (19) 1657-1670.
- [65] Mora-Ochomogo M., and Lohans C. T. (2021)  $\beta$ -Lactam antibiotic targets and resistance mechanisms: from covalent inhibitors to substrates. *RSC Med. Chem.*, 12 (10) 1623-1639.
- [66] Sulistyowaty, M. I., Putra, G. S., Budiati, T., Indrianingsih, A. W., Anwari, F., Kesuma, D., Matsunami, K., & Yamauchi, T. (2023). Synthesis, In Silico Study, Antibacterial and Antifungal Activities of N-phenylbenzamides. *International Journal of Molecular Sciences.*, 24(3), 2745.
- [67] Guengerich F. P. (2024) Cytochrome P450 enzymes as drug targets in human disease. *Drug Metab Dispos.*, 52 (6) 493-497.
- [68] Newsome A. W., Nelson D., Corran A., Kelly S. L., and Kelly D. E. (2013) The cytochrome P 450 complement (CYPome) of *Mycosphaerella graminicola*. *Biotechnol. Appl. Biochem.*, 60 (1) 52-64.
- [69] Sadowski E., Pietrancosta N., Veyron-Churllet R., Boucher J.L., Pionneau C., Clodic G., Matheron L., Poch O., Mayer C., Sachon E., Aubry A. (2025) Characterization of the Orphan Cytochrome P450 CYP135B1 from *Mycobacterium tuberculosis*: Involvement in Metabolism but Not in the Antibacterial Activity of the Antitubercular Drug SQ109. *ACS Infectious Diseases.*, 11 (4), 869-881.
- [70] Balding P. R., Porro C. S., McLean K. J., Sutcliffe M. J., Marechal J. D., Munro A. W., and Visser S. P. D. (2008) How do azoles inhibit cytochrome P450 enzymes? A density functional study. *J. Phys. Chem. A.*, 112 (50) 12911-12918.
- [71] Wang, N., Liu, Y., Jiang, Z., Chen, L., & Liang, X. (2025). Evaluation of the safety of fenbuconazole monomers via enantioselective toxicokinetics, molecular docking and enantiomer conversion analyses. *Journal of Agricultural and Food Chemistry*, 73(16), 9894–9905.

